東北大学機関リポジトリ
TOUR
Tohoku University Repository

Molecular dynamics study on ultrathin liquid water film sheared between platinum solid walls: Liquid structure and energy and momentum transfer

Molecular dynamics study on ultrathin liquid water film sheared between platinum solid walls: Liquid structure and energy and momentum transfer

Daichi Torii[a] and Taku Ohara
Institute of Fluid Science, Tohoku University, 2-1-1 Katahira, Aoba-ku, Sendai 980-8577, Japan

Molecular dynamics simulation has been performed on a liquid film that is sheared in between solid surfaces. As a shear is given to the liquid film, a Couette-like flow is generated in the liquid and energy conversion occurs from the macroscopic flow to the thermal energy, which is discharged back to the solid walls. In such a way, momentum and thermal energy fluxes are present simultaneously. And all these thermal and fluid phenomena take place in highly nonequilibrium state where thermal energy is not distributed equally to each degree of freedom of molecular motion in the vicinities of the solid-liquid interface. In the present paper, platinum and water are employed as solid and liquid, respectively. First, the structure and orientation of water molecules in the vicinities of the solid surfaces are analyzed and how these structure and orientation are influenced by the shear is considered. Based on this result, momentum and thermal energy transfer in the vicinities of and at the solid-liquid interfaces are investigated in detail. Results are compared with those of our previous study, in which monatomic and diatomic molecules are employed as liquid. © *2007 American Institute of Physics*. [DOI: 10.1063/1.2719699]

INTRODUCTION

Liquid film sheared between solid walls exhibits a variety of anomalous thermal and fluid phenomena. As a shear is given to the liquid film, a Couette-like flow is induced in the liquid, and energy conversion occurs from the macroscopic flow to the thermal energy, which is known as viscous heating in the macroscopic sense. The temperature of the liquid rises up, and the generated thermal energy flows back to the solid walls by head conduction. We have been working on such liquid films in order to clarify the characteristics of the energy and momentum transfer both in liquid film and at the solid-liquid interfaces, including the mechanism of viscous heating and energy transfer among the degrees of freedom of molecular motions. The studies are especially focused on liquid films with thickness of a few nanometers, where high shear rate due to the small gap between the solid surfaces influences these phenomena significantly.

It was shown in the previous report of ours for some monatomic and linear molecule liquid films[1,2] that highly nonequilibrium energy distribution (thermal energy not distributed evenly to each degree of freedom of molecular motion) occurred in the liquid just close to the solid surfaces. Significant boundary resistance against fluxes of thermal energy and momentum, with the jumps in temperature and velocity at the solid-liquid interface, was observed, and it was found that the contributions of each degree of freedom of molecular motions to the heat conduction flux were very different from those in bulk liquid. Several crystal planes of the solid walls to contact the liquid film were employed for

comparison in another report of ours[3] and it was clarified that the alignment of the solid atoms of the crystal plane influences the characteristics of energy and momentum transfer significantly.

In the present paper, a liquid film of water contacting platinum solid walls is analyzed. Water is the most promising lubricant because of its environment-friendly nature and its importance in engineering application is increasing more than ever. Another reason to analyze water is a scientific interest. Water molecule has a strong interaction, i.e., hydrogen bond, between themselves, and it also interferes with solid surfaces in various ways, through which some macroscopic characteristics such as hydrophilicity and hydrophobicity are exhibited. These interactions are expected to have a great influence on the thermal and fluid phenomena in the system, and there may be a chance to control the phenomena by selecting the nature of the solid surface.

There are many computer simulation results reported on liquid water film confined between solid surfaces. Zhu and Robinson[4] performed molecular dynamics simulations and investigated the structure and properties of liquid water between two rigid plates. They measured the angle of H–O–H and the value of the dipole moment and found that they are very different from those in bulk liquid. Raghavan *et al.*[5] observed the orientation of liquid molecules on platinum surface in detail. Pertsin and Grunzen[6] showed that the orientation of water molecules on the solid surface influences a lot to the structure and thermal properties in the vicinities of the interface.

In the present study, molecular dynamics simulations of an ultrathin liquid water film sheared between platinum solid surfaces have been performed and thermal characteristics of the system such as transport of thermal energy and thermal

---
[a]Author to whom correspondence should be addressed. Tel.: +81-22-217-5252; Fax: +81-22-217-5252; Electronic mail: torii@microheat.ifs.tohoku.ac.jp
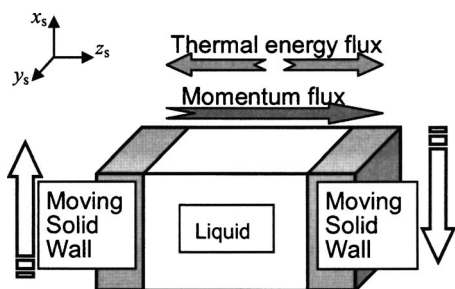
126, 154706-1

FIG. 1. Simulation system and the definition of the spatial coordinates.

TABLE I. Solid walls employed in the simulation.

	Surface molecular number density	Surface crystal plane	Surface molecular configuration	Numbers of atoms in x and y directions	Numbers of layers in z direction
A	Largest	FCC (111)		20×20	7
B	↕	FCC (100)		20×17	8
C		FCC (110)		20×12	11
D	Small			12×20	

boundary resistance at the solid-liquid interfaces were analyzed. For the first half of this paper, the structure and orientation of water molecules in the region close to the solid-liquid interface are investigated, and the influence of the shear on the structure and molecular orientation is clarified. Based on these results, the thermal properties such as temperature distribution, thermal energy flux, and thermal resistance at the interfaces are described and discussed in comparison with those reported for the systems of monatomic and linear molecules as liquid.[1–3]

MOLECULAR DYNAMICS SIMULATION

The simulation system used in the present study is shown in Fig. 1. The system is composed of two parallel solid platinum walls and a thin liquid water film imposed between the walls. Two isothermal solid walls were placed at both ends of the basic cell in the z direction. Periodic boundary conditions were applied in the x and y directions.

To give a shear to the liquid film, the walls were moved at a constant and identical rate (±50 or ±100 m/s) in opposite directions along the x axis. As a result, macroscopic flow momentum was transferred along the z axis in the liquid film, being accompanied by a temperature rise due to viscous heating. The thermal energy generated by the conversion of the flow energy was transferred due to heat conduction from the center region of the liquid film toward the solid walls.

Four types of solid walls were modeled, as shown in Table I. The solid walls were assumed to have the fcc structure. The crystal plane (111), (100), or (110) was in contact with the liquid. For (110) plane, shearing in two directions was applied. These four types are named A–D, respectively. Each solid wall was constructed using 7–11 layers of solid molecules in such a manner that the thickness in the z direction was almost identical for the four types of solid walls. No intentional control of molecular motion, such as temperature control, was applied in the calculation of molecular motion of solid and liquid molecules. However, a kind of Langevin method[7] was applied so as to represent a heat bath at a constant temperature, to model an actual system that involves the part of a solid material, e.g., bearing whose heat capacity is much larger than that of the liquid film. In the method, phantom molecules are placed outside the solid molecule layers and excited by the random force of Gaussian distribution with a standard deviation whose magnitude is determined by the target temperature. The integrated interaction acting on the solid molecules from an isothermal semi-infinite solid is represented by the interaction between the

solid molecules and the phantom molecules. The interaction between solid molecules was modeled using a harmonic potential, with the potential parameters and mass values being those of platinum: the spring constant was 46.8 N/m, the equilibrium distance $r_{eq} = 2.77 \times 10^{-10}$ m, and the mass 3.24 $\times 10^{-25}$ kg. The dimensions of the basic cell in the x and y directions were fixed to ~5.0 nm in every case by arranging 12–20 solid atoms in each direction.

For water, the extended simple point change (SPC/E) potential, which is the most successful potential model that reproduces various thermophysical properties and equation of state of real water, was applied. The heat transfer characteristics and its molecular mechanism of the bulk water using this SPC/E potential have already been analyzed and the contribution of molecular motion and the effect of hydrogen bond were reported by one of the authors.[8] For the potential between a water molecule and a solid molecule, the work of Kandlikar et al.[9] has guided us to utilize the potential developed by Spohr and Heinzinger (SH).[10]

To calculate the Coulomb force, two-dimensional particle-mesh Ewald method,[11] which was developed for calculations of Coulomb interactions in three-dimensional systems with two-dimensional periodicity, was employed, with a fast Fourier transform library FFTW.[12]

The thickness of the liquid film, defined by the distance in the z direction between the time-averaged position of solid molecule layers, each of which contacted the liquid film at each end, was equated to $5\sigma_{oo}$ (1.6 nm), where σ_{oo} is the length parameter for the Lennard-Jones (LJ) potential between oxygen atoms in the SPC/E modeled water. The number of constituent molecules of the liquid film was determined by trial and error in such a way that the pressure of the liquid, which was measured by forces in the z direction acting on the solid walls, was within ±10 MPa so as not to influence the liquid structure.

When a shear is applied to the liquid film, the temperature of the liquid film increases until it reaches a steady state at equilibrium. The value which the liquid film temperature reaches an equilibrium depends on the type of solid wall and
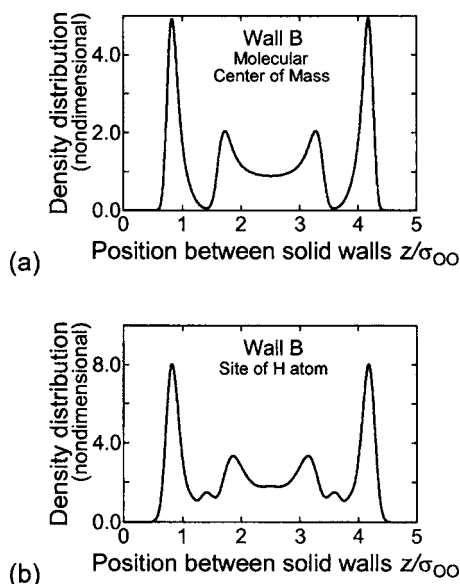
FIG. 2. Number density distribution of (a) center of mass of molecules and (b) hydrogen atoms. (Solid wall B, velocity of the solid walls ±100 m/s.)

FIG. 3. Velocity distributions for the case with (a) solid wall B and (b) solid wall C. (Velocity of the solid walls ±100 m/s.) The series of plots combined by lines in the middle of the graphs are the data averaged over the molecular motions in each layer of liquid molecules shown in Fig. 2(a). There are five molecular layers for the wall C case. The other plots denote the data for solid layers.

the shear rate. In order to eliminate the effect of the difference between the liquid temperatures of the systems studied, the temperature of the phantom molecules in each system was selected in such a way that the average temperature of the first contact layer (see Fig. 2) at the equilibrium state was identical among the systems with various walls and shear rates. The temperature of the first contact layer mentioned here is based on the kinetic energy of liquid molecules due to the translational motion along the z axis (referred to as the z temperature hereafter), although thermal energy is not partitioned equally to all degrees of freedom for molecular motion, as will be described later, and the x, y, and z temperatures are not equal. The average z temperature of the first contact layer was selected to be 300 K.

The data for analyses were obtained by simulations with a time step of 0.5×10^{-15} s for 3 000 000 steps (for measurements of temperatures, momentum, and thermal energy fluxes) or 2 000 000 steps (for others) after an equilibrium state was established by an equilibration run for the preceding 1 000 000 steps.

STRUCTURE AND ORIENTATION OF WATER MOLECULES ADJACENT TO SOLID SURFACE INFLUENCED BY SHEAR

Figure 2 shows number density distributions of water molecules and hydrogen atoms, plotted against the position across the water film. Since the distribution of oxygen atoms is nearly the same as that of molecules, it is not shown here. For the case shown in the figure, solid wall B was employed and the velocities of the solid walls were ±100 m/s, but there was almost no influence of the shear and the profile is similar to other solid walls' cases. Water molecules are trapped by the potential of the solid molecules and form solidlike layered structure for the whole range of the film. Hereafter, we call the layer of liquid molecules that contacts
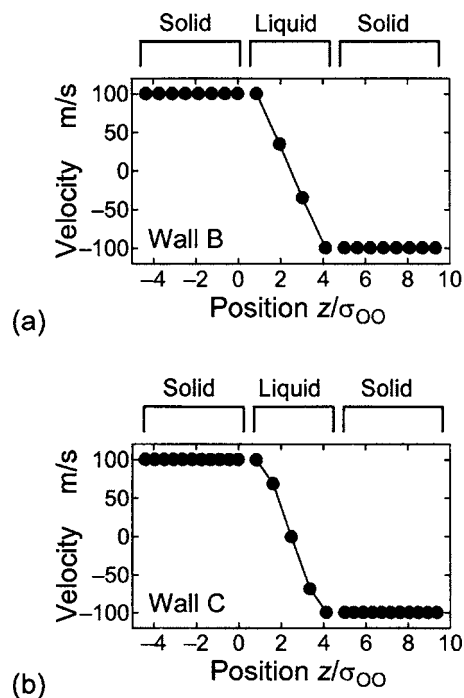
the solid wall as the first contact layer, and the next layer toward the center of the film as the second contact layer.

A Couette-like macroscopic flow was generated in the x direction and its velocity distribution is shown in Fig. 3. The left wall moves at 100 m/s and the right wall at −100 m/s. The velocity difference between the first contact layer and the second contact layer is smaller than that between the layers in the middle of the film for the case with C. This is because the viscosity of water is larger as getting close to the solid wall due to the enhanced solidlike structure. This tendency is also seen for cases with walls A and D. For all cases, the average velocity of the molecules in the first contact layers is almost the same as that of the contacting solid wall, and the velocity slips at the solid-liquid interfaces are very little, which is contrary to the results in our previous study with LJ liquids.[3] The profiles for the case of half the velocity of the solid wall (±50 m/s) are almost the same with the results shown in Fig. 3 except for the magnitude of velocities reduced to a half.

Judging from the nature of the SH potential, it is clear that one water molecule prefers to sit on top of a platinum atom when it is placed alone. For cases with multiple water molecules existing on a surface, it has been revealed by molecular dynamics simulations that each of the water molecules tends to find a platinum atom and stay on top of it when it is close to the surface.[13] In the present study, the influence of the shear to this structure was investigated. Only the molecules in the first contact layer are examined here, and Fig. 4 shows the existence probabilities of their oxygen atoms projected onto the solid-liquid interface. Clear peaks
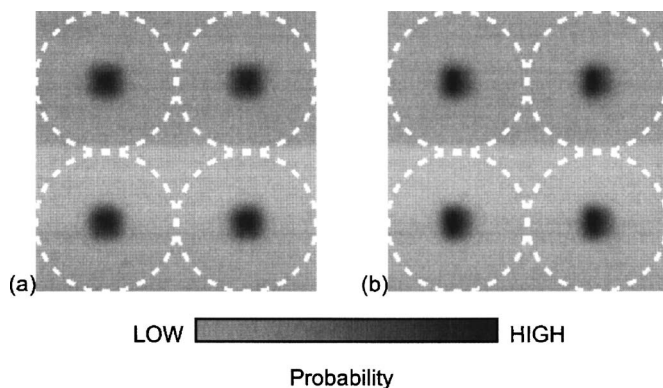
FIG. 4. Probability distributions of the center of mass of water molecules projected onto the surface of the solid wall for the case with wall B. Velocities of the solid walls are (a) 0 m/s and (b) ±100 m/s; the solid wall moves toward the right on this paper. The molecules counted are those existing in the liquid contacting layer. White dotted circles denote outer shapes of platinum atoms on the solid surface.

are observed on each top of platinum atoms. When a shear is applied [Fig. 4(b)], the positions of these peaks are shifted in the direction opposite to the movement of the solid wall. The displacement in the shift of the peaks depends on the types of the solid wall employed and varies between 0.6% and 2.2% of r_{eq} for the case of the wall velocity of ±100 m/s.

In the same way, the existence probability of hydrogen atoms on the solid surface is analyzed in the two images in Fig. 5. Four distinct identical peaks are observed around each platinum atom. When a shear is applied [Fig. 5(b)], on the contrary, the existence probabilities of the peaks become different; the spot on the side of the traveling direction of the wall has a lower probability, and the probability of the other side increases. This indicates that the orientation of the water molecules is influenced by the shear. Further discussion concerning orientation of the molecules will be described later with the probability distributions of some angles. The same tendency as above is observed for the systems with other solid walls.

To investigate the density of the water molecules in the first contact layer, the areal density of those water molecules
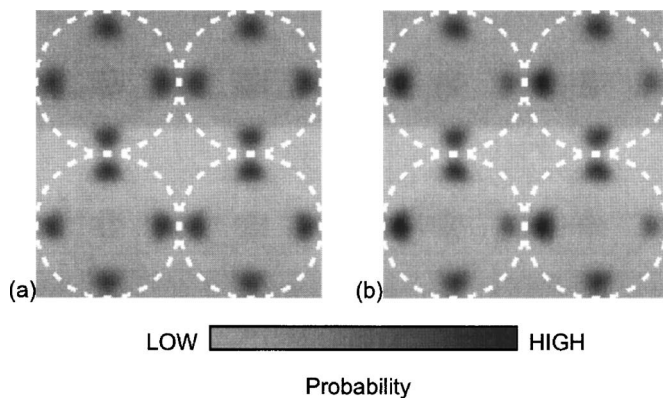

FIG. 5. Probability distributions of hydrogen atoms projected onto the surface of the solid wall for the case with wall B. Velocities of the solid walls are (a) 0 m/s and (b) ±100 m/s; the solid wall moves toward the right on this paper. The hydrogen atoms belonging to the water molecules existing in the liquid contacting layer are counted. White dotted circles denote outer shapes of platinum atoms on the solid surface.

TABLE II. Areal density of water molecules in the first contact layer. The influence of the shear was very little. The values expect for b are all normalized by the density of platinum atoms on the fcc(111) surface (wall A)

Solid wall	Crystal plane contacting liquid	Relative areal density of platinum atoms on crystal plane a	Number of water molecules in first contact layer per platinum atom b	Relative areal density of water molecules in first contact layer ab
A	fcc (111)	1.00	0.82	0.82
B	fcc (100)	0.87	1.00	0.86
C	fcc (110)	0.61	1.03	0.63
D			1.03	0.63

projected onto the solid-liquid interface is calculated and the results are shown in Table II. Here, the areal density is given by the number of molecules per unit area. If all platinum atoms always have one water molecule on each top, the areal density of the water molecule is identical to that of platinum atoms at the crystal plane on the surface. However, the areal density of the platinum atoms on fcc(111) surface is too dense for water molecules to be coupled with all platinum atoms, and only 82% of platinum atoms have their own water molecule on its top. On the other hand, almost all platinum atoms on fcc(100) and (110) surfaces make a pair with a water molecule. Thus, the resulting areal density of water molecules in the first contact layer is largest on fcc(100) surface followed by the cases on (111) and (110), while the areal density of platinum atoms on the surface is in the order of fcc(111)>(100)>(110). No influence of the shear is observed in these findings.

To observe the orientation of water molecules near the solid surfaces, molecular coordinates are defined as in Fig. 6. (Spatial coordinates are defined as shown in Fig. 1.) Figure 7 shows probability distributions of two angles for the case without shear: (a) molecular y axis y_m to spatial z axis z_s and (b) molecular z axis z_m to spatial z axis z_s. For the molecules in the first contact layer, both distributions, (a) and (b), have a peak at $\pi/2$, which indicates that most of the molecules exist with both of their O–H arms parallel to the solid-liquid interface. The figure is the case with wall B, but the case with wall A exhibits the same tendency with comparatively higher peak around the angle of $\pi/2$. This observation result is consistent with the report of Raghavan et al.[5] In the cases with walls C and D, however, the tendency is similar, but the peaks are much lower. As the influence of the shear is little for all cases, no result of the cases with shear is shown here.

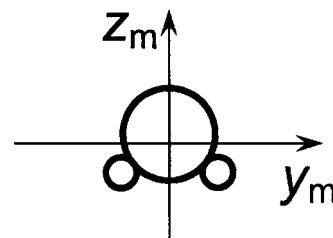Thus, it is revealed that water molecules in the first con-

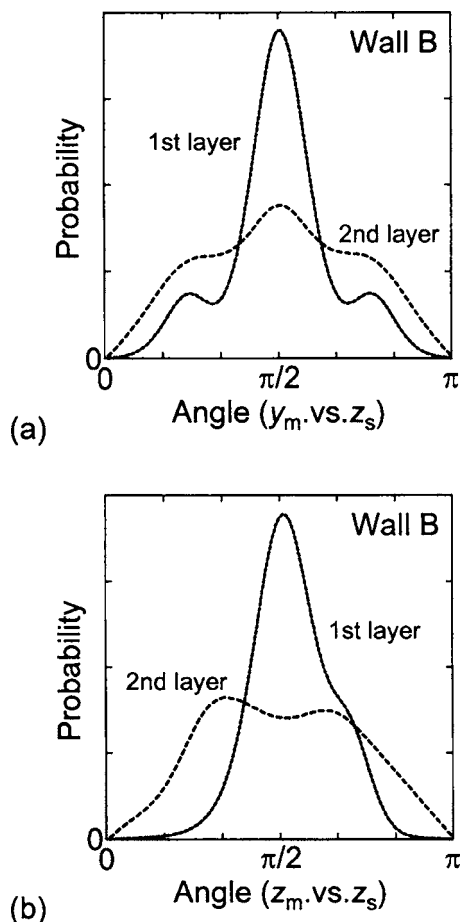FIG. 6. Definition of the molecular coordinates for analyzing the orientation of molecules.

FIG. 7. Probability distributions of orientation of water molecules in each molecular layer: (a) the angle from y_m to z_s and (b) z_m to z_s. "first layer" and "second layer" referred here are those closer to the left solid wall in Fig. 1. (Solid wall B, velocity of the solid walls 0 m/s.)

tact layers are usually on top of a platinum atom with their O–H arms parallel to the solid-liquid interface. Based on these facts, the orientation of molecules to the direction of the shear and influence of the shear on it are shown in Figs. 8 and 9. The angle of the molecular y axis projected to the spatial x-y plane to the spatial x axis is examined and its probabilities are plotted in the figures. The results are shown for the second contact layer as well as the first; however, the discussion below focuses on the orientation of molecules in the first contact layer, since the distribution for the second contact layer is more or less flat and almost no correlation was observed.

In Fig. 8(a) for the case with wall B without shear, four distinct peaks are observed, which are $-(3/4)\pi$, $-\pi/4$, $\pi/4$, and $(3/4)\pi$. According to this result as well as those obtained in Figs. 4 and 7, four water molecules that have the highest probability in position and orientation are illustrated on the solid surface in Fig. 8(c). From this figure, it can easily be estimated that one water molecule creates two hydrogen bonds with the two molecules on the neighboring platinum atoms, although it is not possible for all hydrogen bonds to be "perfect" since the angle H–O–H is about 10° larger than 90°. The positions of the hydrogen atoms in Fig. 8(c) are also consistent with the spots of high probability in Fig. 5. As a result of this hydrogen bond, a hydrogen bond
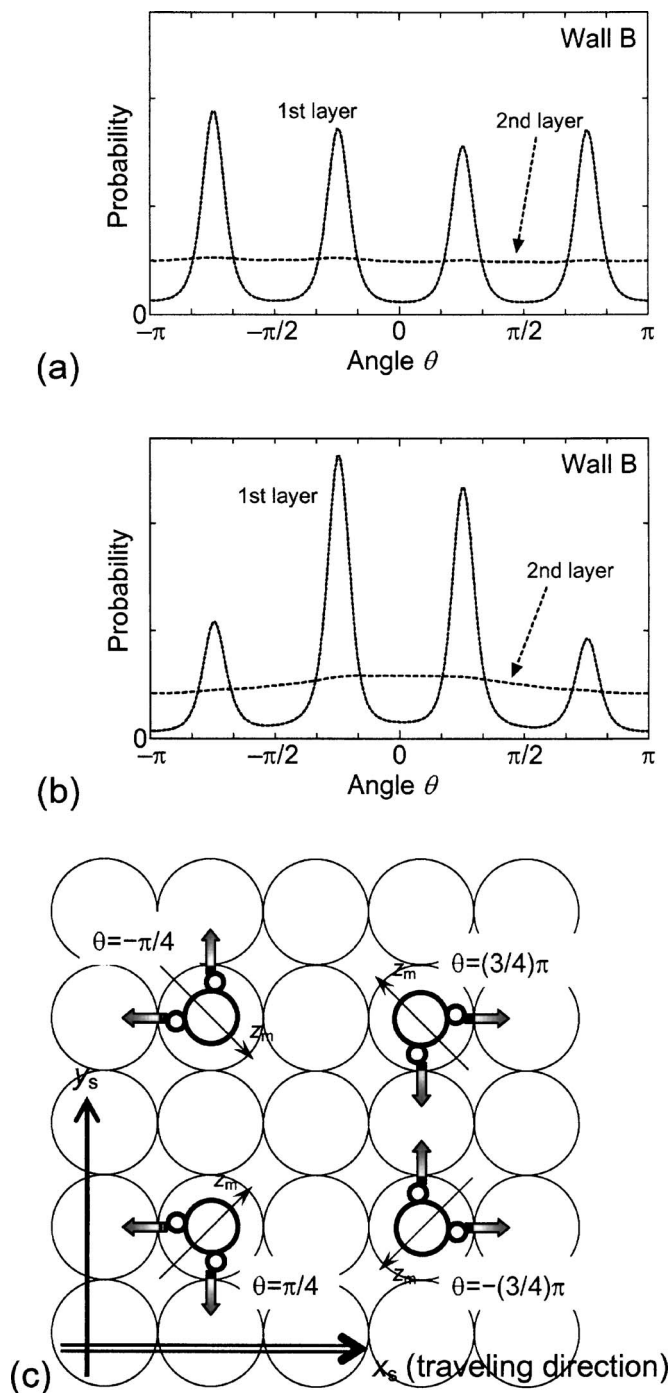

FIG. 8. Probability distributions of orientation of water molecules in each molecular layer. The measured angle θ is z_m projected to x_s-y_s plane to x_s. Velocities of the solid walls are (a) 0 m/s and (b) ±100 m/s. "first layer" and "second layer" referred here are those closer to the left solid wall in Fig. 1. (c) Sketches of the water molecules in the first contact layer with the most probable orientations. Large circles represent platinum atoms, and the thick arrows denote the direction of possible hydrogen bonds. (Solid wall B.)

network, which usually forms a tetrahedral structure, is formed in a flat plane that is parallel to the solid-liquid interface. When the shear is applied, shown in Fig. 8(b), the peaks at $-(3/4)\pi$ and $(3/4)\pi$ decrease while those at $-\pi/4$ and $\pi/4$ increase, which shows that the O to H vector tends to point at the opposite side to the direction of the movement of the solid wall. The reason of this uneven distribution of
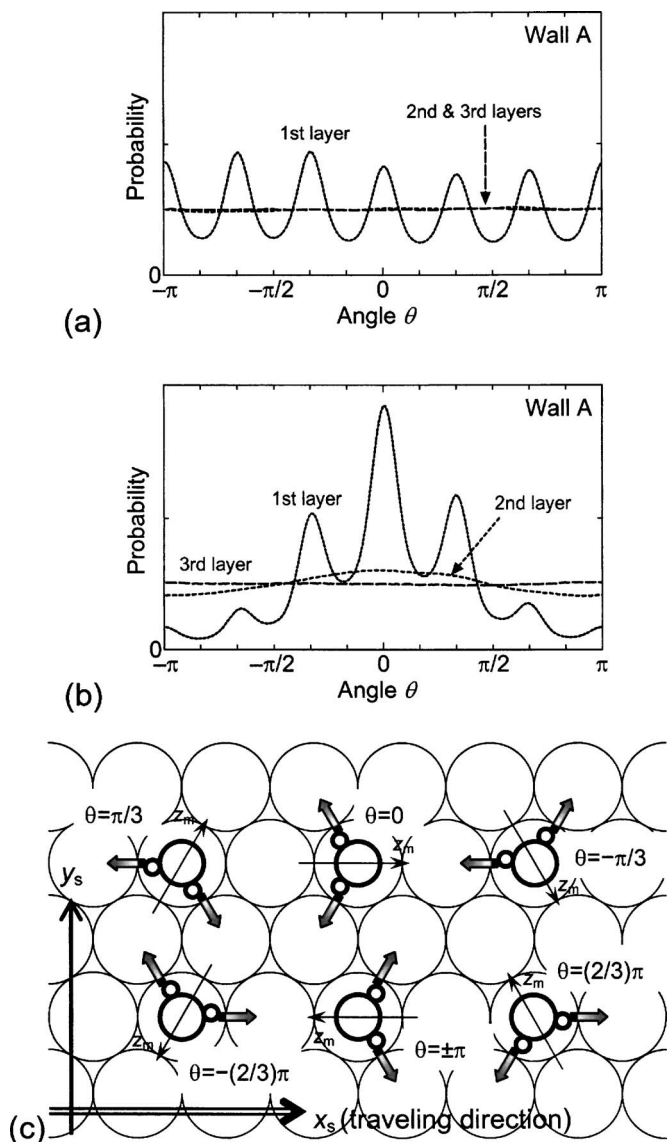
(a)

(b)

(c)

FIG. 9. Probability distributions of orientation of water molecules in each molecular layer. The measured angle θ is z_m projected to x_s-y_s plane to x_s. Velocities of the solid walls are (a) 0 m/s and (b) ±100 m/s. "first layer" and "second layer" referred here are those closer to the left solid wall in Fig. 1. (c) Sketches of the water molecules in the first contact layer with the most probable orientations. Large circles represent platinum atoms, and the thick arrows denote the direction of possible hydrogen bonds. (Solid wall A.)

(a)

(b)

FIG. 10. Distribution of temperature for the case with (a) wall B and (b) wall C. (Velocity of the solid walls ±100 m/s.) Series of plots combined by lines at the center of the graphs denote the data averaged over the molecules belonging to each liquid layer observed in the number density distributions. Series of the other dots denote the data for solid molecule layers.

ENERGY AND MOMENTUM TRANSFER IN WATER FILM AND AT WATER-PLATINUM INTERFACE

The temperature distributions are shown in Fig. 10 for the cases with walls B and C. The temperature corresponding to the translational kinetic energy T^{tr} can be divided into x, y, and z components and they were plotted individually in the graphs. Here, these "temperatures" were calculated from the kinetic energy that was distributed to each degree of freedom of molecular motion. In the same way, T^{rot} is the temperature corresponding to the rotational motion of the molecules. To obtain the temperature for translational motion in the direction of the shear, only the random component of the molecular velocity, which was obtained by subtracting the macroscopic flow velocity from the molecules' gross velocity, was applied. The average temperature of the liquid film is higher than that of the solid walls due to the viscous heating. There is a large temperature difference between the layer of liquid molecules that contacts the solid (first contact layer) and the layer of the solid wall that contacts the liquid. In the solid wall adjacent to the solid-liquid interface, the temperature difference among the three components of T^{tr} is remarkable.

the orientation comes from the interaction between hydrogen and platinum atoms. There is always a repulsive force between these atoms, which decays with increase of the interatomic distance. When the position of the oxygen atom is shifted due to the shear, the hydrogen atoms prefer the position on the same side of the shifts of the oxygen atom simply because the distance between hydrogen and platinum atoms gets farther in that position than in the other side.

Figure 9 shows the results of the same analysis as Fig. 8, but with wall A. The situation and characteristics are the same as described above for wall B, but there are six peaks for wall A, corresponding to the six water molecules drawn in Fig. 9(c). Again, it seems that hydrogen bonds are formed with the two water molecules on the neighboring platinum atoms. The same influence of the shear is also recognized.
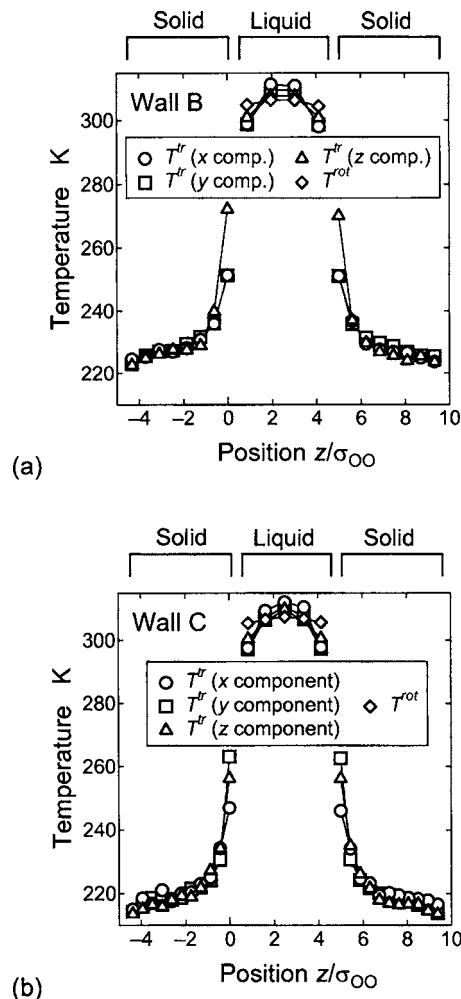
This tells that the thermal energy is not distributed evenly to each degree of freedom of molecular motion, which means that the system is in a highly nonequilibrium state. Furthermore, the distribution of T^{tr} in liquid is roughly parabolic, while T^{rot} shows more uniform temperature distribution for the whole range of the liquid film.

The total energy flux in the z direction that passes through a control surface $J_{tot,z}$ is given by[8]

$$J_{tot,z}S_{xy} = \sum_i \left[\left(\frac{1}{2}m\mathbf{v}_i^2 + \frac{1}{2}I\omega_i^2 + \phi_i \right) \Big/ 1 \right] \frac{v_{i,z}}{|v_{i,z}|}$$
$$+ \frac{1}{2}\sum_i \sum_{j>i} \left[\mathbf{F}_{ij} \cdot (\mathbf{v}_i + \mathbf{v}_j) + \mathbf{N}_{ij} \cdot \boldsymbol{\omega}_i \right.$$
$$\left. - \mathbf{N}_{ji} \cdot \boldsymbol{\omega}_j \right] \frac{z_{ij}}{|z_{ij}|}, \tag{1}$$

where S_{xy} is the area of the control surface. m and $\mathbf{v}_i$ denote the mass and velocity of molecule i, respectively. I and ω are moment of inertia and angular velocity, respectively, and ϕ_i is the potential energy of molecule i. $\mathbf{F}_{ij}$ and $\mathbf{N}_{ij}$ are intermolecular forces between molecules i and j, and torque vector acting on molecule i due to its interaction with molecule j, respectively, where z_{ij} is the distance along the z axis between molecules i and j. The first term on the right side of Eq. (1) represents the transport of energy of molecules themselves due to their motion; the summation is made over the molecules that pass through the control surface in a unit period of time. The second term represents the energy transfer due to changes of molecular energy caused by intermolecular forces acting between a pair of molecules; the double summation is made over all pairs of molecules which hold the control surface between them at a certain moment. In this second term, $\mathbf{F}_{ij} \cdot (\mathbf{v}_i + \mathbf{v}_j)$ represents the contribution of the translational motion, which is referred to hereafter as translational energy transfer. The term $\mathbf{N}_{ij} \cdot \boldsymbol{\omega}_i - \mathbf{N}_{ji} \cdot \boldsymbol{\omega}_j$ represents the contribution of the rotational motion, i.e., rotational energy transfer.

The total energy flux given by Eq. (1) involves both the transfer of the macroscopic flow energy and the thermal energy. The thermal energy flux that is equivalent to heat conduction flux in the macroscopic limit is obtained by using the random component of molecular velocity instead of the entire molecular velocity. The velocity vector $\mathbf{v}$ of a molecule is divided into the macroscopic flow velocity $\bar{\mathbf{v}}$ and the random component $\mathbf{v}'$, and substitution of $\mathbf{v}$ in Eq. (1) by $\bar{\mathbf{v}}$ gives the thermal energy flux $J_{therm,z}$.

$$J_{therm,z}S_{xy} = \sum_i \left[\left(\frac{1}{2}m\mathbf{v}_i'^2 + \frac{1}{2}I\omega_i^2 + \phi_i \right) \Big/ 1 \right] \frac{v_{i,z}}{|v_{i,z}|}$$
$$+ \frac{1}{2}\sum_i \sum_{j>i} \left[\mathbf{F}_{ij} \cdot (\mathbf{v}_i' + \mathbf{v}_j') + \mathbf{N}_{ij} \cdot \boldsymbol{\omega}_i \right.$$
$$\left. - \mathbf{N}_{ji} \cdot \boldsymbol{\omega}_j \right] \frac{z_{ij}}{|z_{ij}|}. \tag{2}$$

In most cases of liquids, the second term on the right side of Eq. (2) dominates the first term.[8] This tendency is promoted by locating the control surfaces at local minima of the num-
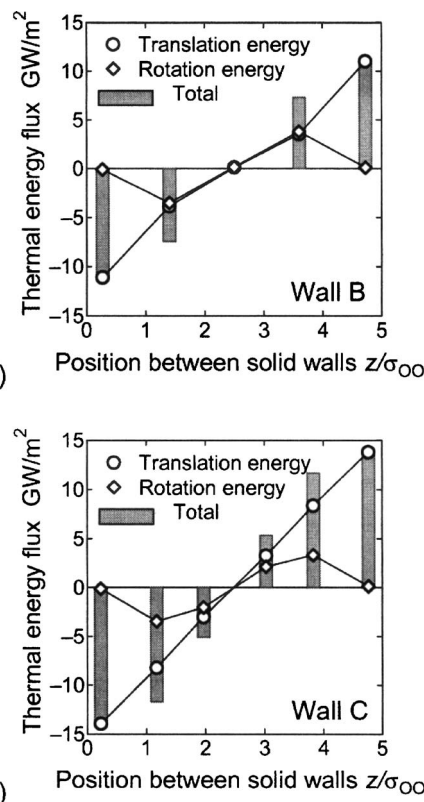

FIG. 11. Contributions of the translational and rotational motions to the thermal energy flux in the liquid film and at the interfaces for the case with (a) wall B and (b) wall C. (Velocity of the solid walls ±100 m/s.) Rightmost and leftmost bars and plots are the data at solid-liquid interfaces, and other data are measured at control surfaces in the liquid film. The control surfaces are parallel to the xy plane and their z positions are at the local minima of the number density distribution of water molecules (see Fig. 2).

ber density distribution, because there are little molecules that go over the control surfaces. Therefore, only the second term is analyzed for the thermal energy flux in the rest of the present paper.

Figure 11 shows the thermal energy flux calculated by Eq. (2), observed at solid-liquid interfaces and in the liquid film. The contribution of rotational energy transfer in bulk water has already been analyzed by one of the authors to be approximately 65%.[8] In the present case, however, the rotational energy transfer contributes less as getting closer to the solid-liquid interface, and there is no contribution at all at the solid-liquid interface. This is because the interaction between a hydrogen atom and a platinum atom is relatively weak and oxygen atom is too close to the center of mass of water molecule. Therefore the rotational motion of the water molecules cannot excite the motion of platinum atoms very well. This observation holds true regardless of the types of solid walls employed.

The contributions of translational energy transfer and rotational energy transfer can further be decomposed into three components that correspond to the degrees of freedom of translational motion of the molecules. In Fig. 12, the translational thermal energy transfer is plotted with its three components according to the molecular motions parallel to x_s, y_s, and z_s axes. The total is identical to the data plotted with circle marks in Fig. 11. For all cases, the components of the
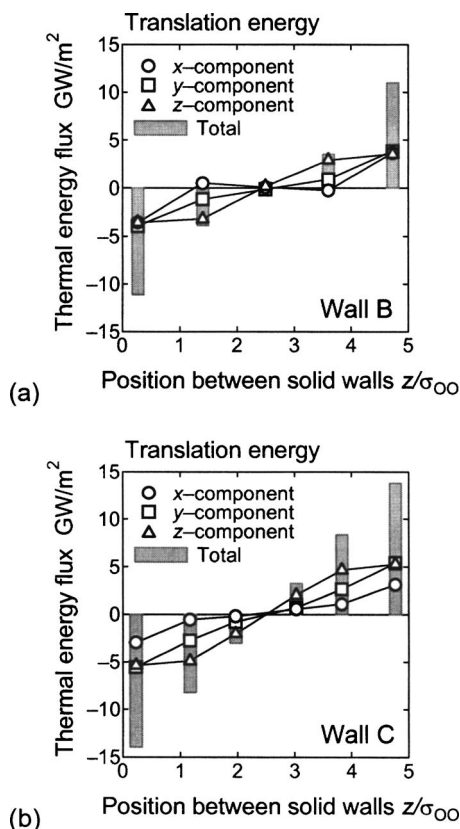
FIG. 12. Contributions of the molecular motions of each degree of freedom to the thermal energy flux due to translational motion of molecules observed in the liquid film and at the solid-liquid interfaces for the case with (a) wall B and (b) wall C. (Velocity of the solid walls ±100 m/s.)
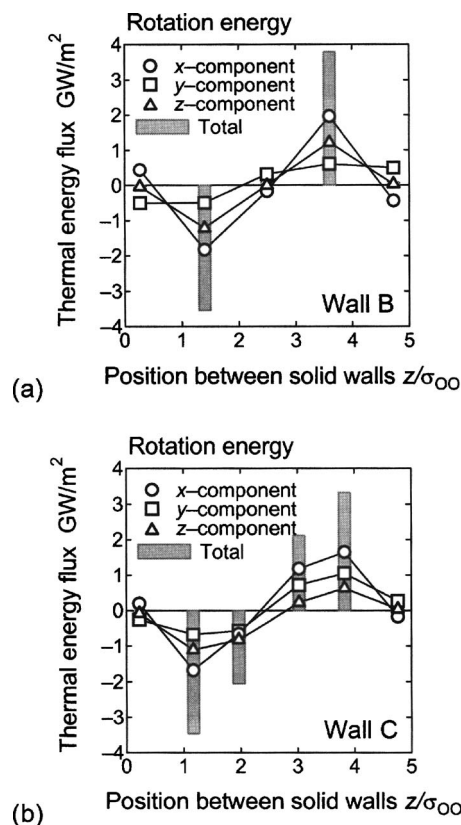
FIG. 13. Contributions of the molecular motions of each degree of freedom to the thermal energy flux due to rotational motion of molecules observed in the liquid film and at the solid-liquid interfaces for the case with (a) wall B and (b) wall C. (Velocity of the solid walls ±100 m/s.)

molecular motions parallel to the interface (x and y components) contribute as well as the other (z) component at solid-liquid interfaces, in contrast to the fact that they contribute little when the alignment of the platinum atom on the solid surface is dense in the corresponding direction for the case with LJ liquids.[3] This difference comes from the solid-liquid intermolecular potential. In the case of LJ liquids, the molecules prefer to stay in hollow sites on the potential surface of solid molecules when they contact the solid surface. The potential surface made by solid molecules is smoother in the case of solid surfaces where molecules are packed with higher density than that in the case of solid surfaces with lower molecular density. So, larger number of surface molecules makes the energy transfer by the motion of molecules parallel to the interface more difficult, which results in smaller contributions of these motions. For the case of water, on the other hand, liquid molecules stay on top of the solid molecules regardless of the area density of molecules on the solid surface. The potential surface is rough according to a positional change parallel to the interface even in the cases with solid surfaces with highly packed molecules. This is the reason why molecular motion parallel to the interface contributes well to energy transfer for water case.

The y component contributes larger than x component at solid-liquid interfaces for the case with wall C. Although the result is not shown here, y component is larger than x component for the case with wall D. Note that the x direction of wall C and y direction of wall D are the same directions on

fcc(110) plane (see Table I). This promoted energy transfer by the molecular motion along the y axis for wall C and x axis for wall D is consistent with the relatively smaller temperature jumps in those components at solid-liquid interfaces in Fig. 10.

Figure 13 shows the rotational energy transfer and its three components according to the rotational motions around x_s, y_s, and z_s axes. Although the total rotational energy transfer is zero at the interfaces, x and y components have values and they cancel each other to be zero in total. It is worth to be noted that the x component and y component exhibit the opposite characteristics at the solid-liquid interface for the case with B, and this is nothing else but the influence of the shear, because x and y directions of wall B are identical in structure.

Velocity jump at the solid-liquid interface was defined as the velocity difference between the solid wall and the extrapolated flow velocity of the liquid film at the interface. Here, the interface was defined as the plane parallel to xy plane, whose z position divided the distance between the averaged position of the layer of solid molecules and that of liquid molecules which contacted each other with a ratio of r_{water} to r_{eq}. Here, r_{water} is 2.8×10^{-10} m, which is the equilibrium distance between two water molecules in the SPC/E liquid water at 300 K. To extrapolate the macroscopic flow velocity, the flow velocity distribution was approximated by the equation
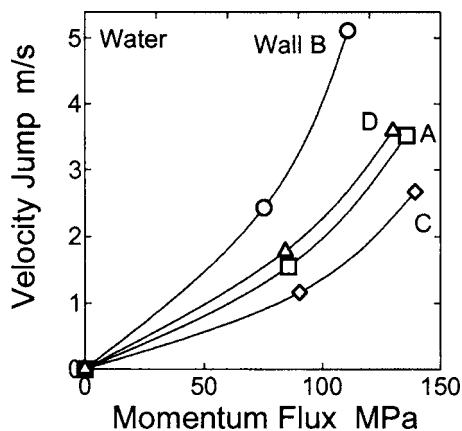
FIG. 14. Velocity jump vs momentum flux at solid-liquid interfaces.

$$v_x(z) = -v_w \tanh\left(\alpha\left(z - \frac{L_{\text{liq},z}}{2}\right)\right), \qquad (3)$$

where $L_{\text{liq},z}$, α, and v_w denote the thickness of the liquid film, the fitting parameter, and the velocity of the solid wall, respectively.

Momentum flux is calculated in a similar way as energy flux. Regarding the momentum in the x direction, its flux that passes through a control surface S_{xy} in the direction of z is calculated by[14]

$$P_{xz}S_{xy} = \sum_i (mv_{i,x}/1)\frac{v_{i,z}}{|v_{i,z}|} + \sum_i \sum_{j>i} F_{ij,x}\frac{z_{ij}}{|z_{ij}|}, \qquad (4)$$

where P_{xz} is the momentum flux.

Figure 14 shows the correlation between the momentum flux and the velocity jump at solid-liquid interfaces for each kind of solid walls employed. The plotted data include the simulation results for the cases with the speed of the solid walls of ±50 m/s. The velocity jump exhibits a nonlinear response to momentum flux; the gradient of the curves increases as the momentum flux increases. Clear differences among the four types of solid walls are observed, although the difference is not very large as compared with the case of monatomic and linear molecules as the liquid.[3]

Figure 15 shows the correlations between temperature jump and thermal energy flux at solid-liquid interfaces. The temperature jump, which is defined as the temperature difference between the first contact layer of liquid molecules and the contact layer of the solid molecules, was obtained for three degrees of freedom, x, y, and z. The thermal energy flux passing through the solid-liquid interface can be divided into the contributions of translational motion of molecules in the corresponding three degrees of freedom. Figure 15(b) is the plot for each individual component and Fig. 15(a) shows the relation of average temperature jump against the total thermal energy flux. The gradient of the line in Fig. 15(a) indicates thermal resistance in a macroscopic sense. In accordance with the concept of the resistance, thermal resistance for each component in Fig. 15(b) is defined by the gradient of each straight line. In Fig. 15(b), the two components that have the smallest thermal resistance are the y component of wall C and the x component of wall D, which are the identical direction on the same fcc(110) plane. The other direc-
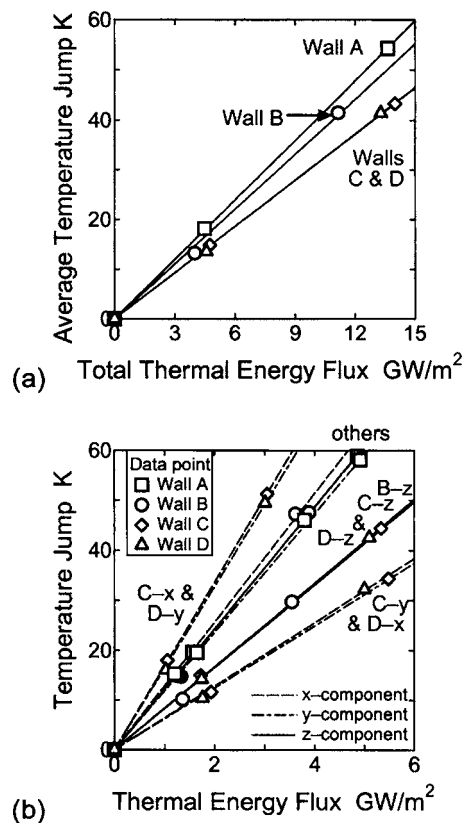

FIG. 15. (a) Average temperature jump vs thermal energy flux at solid-liquid interfaces. (b) Temperature jump vs thermal energy flux for each degree of freedom at solid-liquid interfaces.

tion parallel to the interface on fcc(110) plane is the y component of wall C and the x component of wall D, and these components have the largest thermal resistance. These two extreme characteristics on fcc(110) plane cause different contributions between x and y components in Fig. 12(b) and different amounts of temperature jumps between x and y in Fig. 10(b). In addition to such characteristics of the thermal resistance for each component, the extent of the contribution of each component to the total thermal energy flux is another factor to define the total thermal resistance shown in Fig. 15(a).

CONCLUSION

Molecular dynamics simulation has been performed on an ultrathin liquid water film confined between two solid platinum surfaces. The structure and orientation of water molecules near the platinum surface are analyzed and the influence of the shear is investigated. Water molecules tend to be on top of platinum atoms, forming a hydrogen network parallel to the interface. By the shear applied, hydrogen atoms prefer to point downstream of the movement of the solid wall, which implies that the orientation of water molecules can be controlled by shear.

Based on these results, the thermal properties of the system were investigated. The contribution of rotational motion to the thermal energy flux was zero at the solid-liquid interface, whereas it occupies 65% in bulk liquid water. Due to the potential of water molecule to take "top site" on platinum

surface, the alignment of the platinum atoms on the solid surface does not have significant influence on the characteristics of energy and momentum transfer at the solid-liquid interface, unlike the case of liquids of monatomic and diatomic molecules.

ACKNOWLEDGMENTS

[1] T. Ohara and T. Yatsunami, Microscale Thermophys. Eng. **7**, 1 (2003).
[2] T. Ohara and D. Torii, Microscale Thermophys. Eng. **9**, 265 (2005).
[3] T. Ohara and D. Torii, J. Chem. Phys. **122**, 214717 (2005).
[4] S.-B. Zhu and G. W. Robinson, J. Chem. Phys. **94**, 1403 (1991).
[5] K. Raghavan, K. Foster, K. Motakabbir, and M. Berkowitz, J. Chem. Phys. **94**, 2110 (1991).
[6] A. Pertsin and M. Grunze, J. Phys. Chem. B **108**, 1357 (2004).
[7] P. Yi, D. Poulikakos, J. Walther, and G. Yadigaroglu, Int. J. Heat Mass Transfer **45**, 2087 (2002).
[8] T. Ohara, J. Chem. Phys. **111**, 6492 (1999).
[9] S. G. Kandlikar, S. Maruyama, M. E. Steinke, and T. Kimura, Proceedings of the ASME Heat Transfer Division 2001: Presented at the 2001 ASME International Mechanical Engineering Congress and Exposition, November 11–16, 2001, New York, New York, Vol. 1, 343 (2001).
[10] E. Spohr and K. Heinzinger, Ber. Bunsenges. Phys. Chem. **92**, 1358 (1988).
[11] M. Kawata, M. Mikami, and U. Nagashima, J. Chem. Phys. **116**, 3430 (2002).
[12] M. Frigo and S. Johnson, Proceedings of the ICASSP Conference, 1998 (unpublished), Vol. 3, p. 1381 (DSP4.7), http://www.fftw.org/
[13] K. Raghavan, K. Foster, and M. Berkowitz, Chem. Phys. Lett. **177**, 426 (1991); T. Kimura and S. Maruyama, The Sixth ASME-JSME Thermal Engineering Joint Conference, 2003 (unpublished), Paper No. TED-AJ03–183.
[14] T. Ohara and D. Suzuki, Microscale Thermophys. Eng. **5**, 117 (2001).